

Mueller matrix polarimetry for differentiating characteristic features of different materials (wood, shinning steel, unpolished plastic)

S. Batool^{*(1)(2)}, M. Nisar⁽¹⁾⁽²⁾, F. Mangini⁽¹⁾⁽³⁾, F. Frezza⁽¹⁾⁽²⁾ E. Fazio⁽¹⁾⁽²⁾

(1) Department of Information Engineering, Electronics and Telecommunications, “La Sapienza” University of Rome, Via Eudossiana 18, 00184 Rome, Italy

(2) Department of Fundamental and Applied Sciences for Engineering, “La Sapienza” University of Rome, Via A. Scarpa 16, 00161 Roma, Italy

(3) Department of Information Engineering, University of Brescia, Via Branze 59, 25123 Brescia, Italy



Abstract

Polarization measurements improve the imaging contrast by using various samples (wood, shinning steel, unpolished plastic). For better explanations of the micro- and macro-structures and basic characteristics of the materials, we perform Mueller matrix imaging on various samples, expressed by the characteristic features of the 3×3 Mueller matrix elements. This research gives new ideas for various samples on the contrast mechanisms of Mueller matrix components, which can provide new diagnostic techniques for biomedical applications.

1 Introduction

Mueller matrix polarimetric imaging is a very potent approach that is extensively used nowadays in many different areas like biomedical applications [1], materials characterization [2], remote sensing [3, 4] etc.. Mueller matrix imaging technique has also tested several clinical applications [5, 6, 7]. While it is commonly mentioned, how the polarization states are converted from the incident into the reflected light, a Mueller matrix shows some details information of reflected light and structural properties of the materials. To address this issue, 3×3 Mueller matrix elements have been calculated, which derive a set of polarization parameters with specific physical meanings, such as Linear Extinction (LE), Depolarization (D), Circular Retardance (CR), and Transmission (T) [8, 9, 10]. Mueller matrix polarimetry is deemed very useful to characterize different natural and man-made materials. In our work, we study different flat samples: wood Horizontal (H), wood Vertical (V), shinning steel Horizontal (H), shinning steel Vertical (V) and unpolished plastic. For this, we need a realistic experimental polarization imaging approach for material identification and comparison between all samples. The ultimate goal of this study is to express the optical behavior of veins, arteries, and nerves for the biomedical diagnosis. For the sake of simplicity, we investigated flat objects in order to understand thoroughly the light scattering effects for its material characteristics. We are assuming that the char-

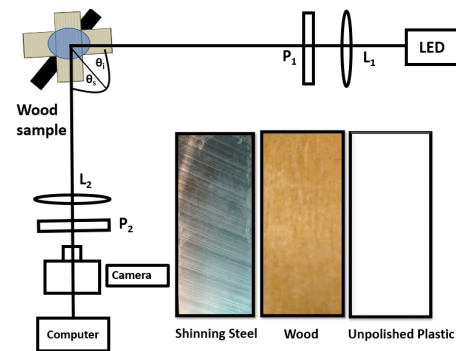


Figure 1. Experimental Setup

acteristic features of wood (H-V) and shinning steel (H-V) may be associated to nerves and arteries respectively and characteristic features of unpolished plastic may be associated to veins.

2 Experimental Setup

We study different samples, wood (H-V oriented), shinning steel (H-V oriented) and unpolished plastic flat samples have been illuminated by linearly polarized light shown in Fig. 1. The wavelength of illumination is 450 nm from a LED, which is collimated by a lens L_1 and then propagates through a linear polarizer P_1 . The samples were illuminated orthogonally, observed at different large angles in order to see the behavior of light according to the respective angle. Backscattered light in terms of photons from the sample passes through the lens L_2 and second polarizer P_2 . Finally, images were captured by a camera, which is connected to the computer. The images were mathematically inspected, to determine the properties of the light diffused towards the observer. In our experimental setup, both polarizers P_1 and P_2 can rotate around their optical axis to vary polarization angles for illumination θ_i and detection θ_s , showed in Fig. 1.

We captured a series of images $I(\theta_i, \theta_s)$, for incident po-

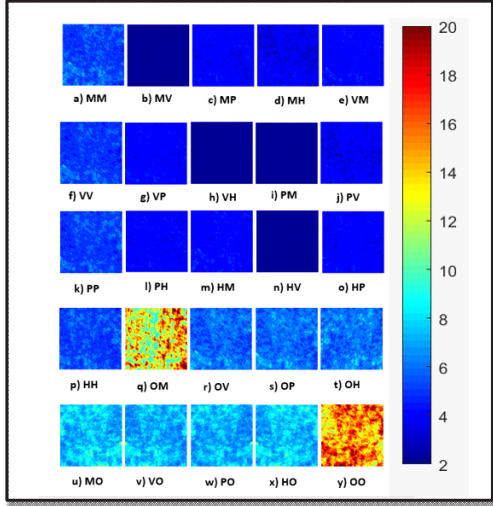


Figure 2. Images for shinning steel-H sample with respect to the 10° angle of observation. By using these images, we can derive 3×3 Mueller matrix elements. Last image (y) shows high intensity of light rather than other all images, because unpolarized light directly fall on the sample. From (p) to (x) images are more bright rather than others, because we have been recorded these images using only one polarizer

larization set of angles $\{315^\circ, 0^\circ, 45^\circ, 90^\circ\}$ using P_1 . We took four images by setting P_2 at $\{315^\circ, 0^\circ, 45^\circ, 90^\circ\}$ corresponding to each incident polarization. In this way, we recorded sixteen images for each sample with respect to different angles of observation. Meanwhile first polarizer P_1 has been removed from our experimental setting, we took again four images by rotating the second polarizer P_2 according to the set of angles $\{315^\circ, 0^\circ, 45^\circ, 90^\circ\}$. We embedded the first polarizer P_1 and removed the second polarizer in the experimental setup, we took four images using the first polarizer P_1 with same set of angles. Finally, we captured one image without using both polarizers P_1 and P_2 . In this way, we recorded total of twenty-five images for each samples shown in Figs. 2, 3.

3 Mueller matrix polarimetry

Polarimetry is the measurement technique, that can be applied for interpretation of the polarization of light. In general, when the light interacts with optical elements that include polarizers, filters, lenses surfaces, scattering media etc, it can change the state of its polarization. This interaction with any optical element or material can be defined as a multiplication of the Stokes vector with a 4×4 matrix, $S' = MS$. The Stokes matrix is modified in terms of Mueller can be written as [1]:

$$\begin{bmatrix} I_{out} \\ Q_{out} \\ U_{out} \\ V_{out} \end{bmatrix} = \begin{bmatrix} m_{11} & m_{12} & m_{13} & m_{14} \\ m_{21} & m_{22} & m_{23} & m_{24} \\ m_{31} & m_{32} & m_{33} & m_{34} \\ m_{41} & m_{42} & m_{43} & m_{44} \end{bmatrix} \begin{bmatrix} I_{inp} \\ Q_{inp} \\ U_{inp} \\ V_{inp} \end{bmatrix} \quad (1)$$

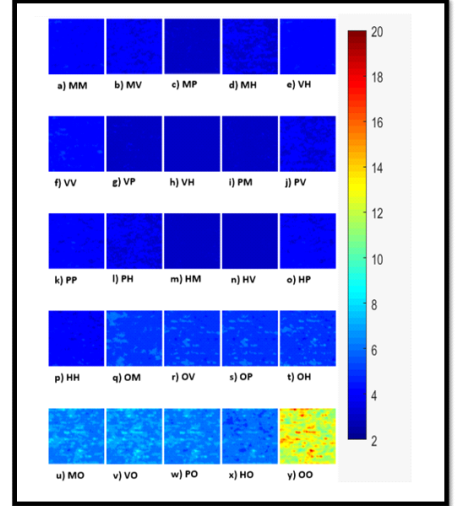


Figure 3. Images for wood-V sample with respect to the 10° angle of observation. By using these images, we can calculate 3×3 Mueller matrix elements. Images represents the input to output intensity of light.

3.1 Physical interpretation of Mueller matrix

Mueller matrix elements can be determined experimentally with different orientations of polarizers illustrated in Fig. 4. The element m_{11} gives the information of the unpolarized light input to output intensity, so this factor can be interpreted as a simple transmission. m_{12} is obtained by measuring the total reflected intensity for horizontal input polarization and subtracting the total reflected intensity for vertical input polarization from it. m_{12} can be expressed as the Linear Extinction (LE) at $0^\circ/90^\circ$. Similarly, m_{21} refers to degree of linear polarization of the scattered light; m_{22} refers the depolarization of input polarization. m_{23} and m_{32} express the Circular Retardance (CR) with opposite sign.

4 Discussion and Conclusions

In our experiment, we have been calculated the 3×3 Mueller matrix, for the characterization of selected samples wood (H-V), shinning steel (H-V), unpolished plastic, at observation angle θ_s varying from 10° to 70° . We have taken an average of three repeated measurements for each sample and normalized all the obtained matrix elements.

During our numerical assessment and elaborations, we have observed the following features of each sample as illustrated in Fig 5. First, we can see that the Mueller matrices for all samples are non-diagonal. Further, the magnitude of the diagonal elements m_{22} and m_{33} is not equal. For the case of shinning steel sample are distributed along both orientations horizontal (solid blue line) and vertical (solid red line), leading to a larger value of the diagonal elements m_{22} and m_{33} as compared to the other samples wood-V (dot red line), wood-H (dot blue line), and unpolished plastic (solid

m_{11}	oo	
m_{12}	$(HO-VO)/2$	
m_{13}	$(PO-MO)/2$	
m_{21}	$(OH-OV)/2$	
m_{22}	$(HH-VV)/4-(HV-VH)/4$	
m_{23}	$(HH+VV)/4-(HV-VH)/4$	
m_{31}	$(OP-OM)/2$	
m_{32}	$(HP+VM)/4-(HM-VP)/4$	
m_{33}	$(PP+MM)/4-(PM+MP)/4$	

Figure 4. Formation of Mueller matrix elements.

green line). For example, the unpolished plastic has smaller diagonal elements m_{22} and m_{33} approaches to zero as compare to all other samples shining steel (V-H), and wood (V-H). Wood-V has higher value of diagonal elements m_{22} and m_{33} as compared to wood-H shown in (Figs. 5, d, h). The abundance of cellulose in wood is the cause of notable absorption, and results in larger values of diagonal elements of wood as compared to the unpolished plastic. The element m_{31} is zero for all samples (see Fig. 5, f), but the element m_{13} displays minimum values rather than zero (see Fig. 5, b). m_{23} and m_{32} show wood-V has superior peaks in plots as compare to shining steel-V. Similarly, the numerical values of wood-H are leading to shining steel-H and unpolished plastic. So, its graphical representation is fluctuated in entire range of observation angle (see Fig. 5, e, g). m_{12} represents the wood (V-H) samples have higher magnitude rather than shining steel(V-H) and unpolished plastic (see Fig. 5, a).

It can be notices that, m_{22} and m_{33} are more sensitive elements for the identification of the shining steel (V-H), wood (V-H), and unpolished plastic samples. This information confesses us to conclude that the change in polarization state of light after interaction with wood and shining steel plays significant role, which can also contribute in its detection. Shinning steel-V and wood-V have more significant numerical results rather than wood-H shining steel-H, and unpolished plastic.

5 Conclusions

In this paper, we apply polarization imaging technique on shining steel-H, shining steel-V, wood-H, wood-V, unpolished plastic to demonstrates the different microscopic aspects of the samples. Using 3×3 Mueller matrix, we have been discussed the polarization parameters such as: Linear Extinction (LE), Depolarization (D), Circular Retardance (CR), and Transmission (T). These parameters are used to identify the characteristic features of the selected samples.

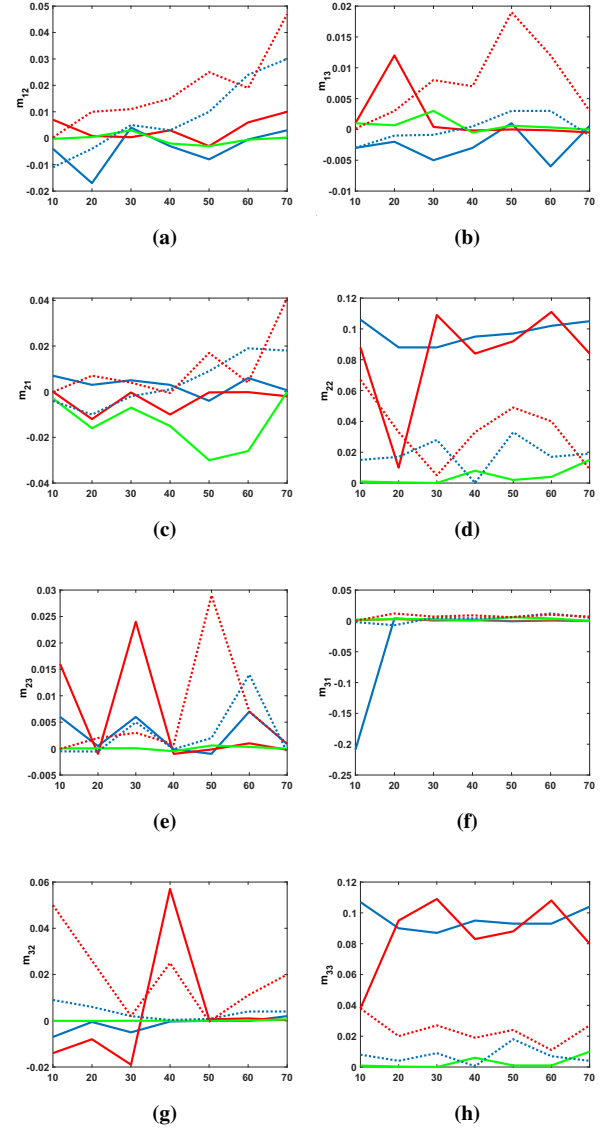


Figure 5. Mueller Matrix elements m_{ij} for all flat samples: wood fibers of two orientation horizontal (dot blue line) and vertical (dot red line), shining Steel H-orientation V-rifling (solid blue line), shining Steel V-orientation H-rifling (solid red line) and the unpolished plastic (solid green line) as functions of the observation angles along $x - axis$.

The experimental and simulation results confirm that the Mueller matrix elements m_{22} and m_{33} are more responsive for the entire range of observation angles in all samples. The main objective of the study is to understand the different behaviour of isotropic and anisotropic materials. So, we consider wood and shinning steel as anisotropic samples, and unpolished plastic is isotropic sample. We can say, that wood and shinning steel shows more sensitiveness towards the polarization state of light. unpolished plastic is isotropic in general as it has no texture, so it is independent of orientation. We notices that, it does not depict active response towards any polarization state. It can be stated as the Mueller matrices elements over the entire observation angle reveal the characteristics of materials using light scattering phenomena. In future, we propose to extend these derived formations for biological samples.

References

- [1] Batool S., Nisar M., Mangini F., Frezza F., Fazio E., "Scattering of Light from the Systemic Circulatory System", *Diagnostics* **10**, 2020 1026.
- [2] Batool S., Nisar M., Mangini F., Frezza F., Fazio E., "Polarization Imaging for Identifying the Microscopical Orientation of Biological Structures", *InProceedings of the URSI GASS Conference*, Rome, Italy 2020 Aug (Vol. 29).
- [3] Batool S., Frezza F., Mangini F., Simeoni P., "Introduction of Radar Scattering Application in Remote Sensing and Diagnostics". *Atmosphere*. **11**, 2020, 517.
- [4] Tyo J. S., Goldstein D. H., Chenault D. B., Shaw J. A., "Polarization in remote sensing-introduction", *Applied optics*, **22**, 2006, 5451-2.
- [5] Fazio E., Batool S., Nisar M., Mangini F., Frezza F., "Recognition of bio-structural anisotropy by polarization-resolved imaging", *Biophysical Review*(submitted).
- [6] Zaffar M., Pradhan A., "Assessment of anisotropy of collagen structures through spatial frequencies of Mueller matrix images for cervical pre-cancer detection", *Applied Optic*, **59**, 2020, 1237-48.
- [7] Yu X., Zhang S., Olivo M., Li N., "Micro-and nano-fiber probes for optical sensing, imaging, and stimulation in biomedical applications", *Photonics Research*, **8** 2020, 1703-24.
- [8] Du E., He H., Zeng N., Sun M., Guo Y., Wu J., Liu S., Ma H., "Mueller matrix polarimetry for differentiating characteristic features of cancerous tissues", *Journal of biomedical optics*, **19**, 2014, 076013.
- [9] Batool S., Nisar M., Mangini F., Frezza F., Fazio E., "Interpreting Mueller Matrix of Anisotropic Material", *In2020 15th European Conference on Antennas and Propagation (EuCAP) 2021 Mar 22*, Dusseldorf, Germany, IEEE, 1-4.
- [10] Batool S., Nisar M., Mangini F., Frezza F., Fazio E., "To study the Mueller matrix polarimetry for the characterization of wood and Teflon flat samples", *Optics communication* (submitted).